DOI: 10.61782/fa.2023.0662

forum acusticum 2023

PREDICTING THE ACOUSTICS OF ARCHTOP GUITARS USING AN AI-BASED ALGORITHM TRAINED ON FEM SIMULATIONS

Giacomo Longo **Sebastian Gonzalez*** **Fabio Antonacci**
Augusto Sarti
DEIB, Politecnico di Milano, Italy

ABSTRACT

In this paper we implement a method that combines finite element analysis and artificial intelligence (AI) to study how the choice of some design and material parameters affects the vibroacoustic response of an archtop guitar. More specifically, we build a dataset varying the geometry (thickness profile of the top plate) and the material properties of the archtop guitar in a parametric fashion. This dataset is the input for a finite element analysis estimating the bridge admittances, directivity and the emitted sound pressure level. An AI-based approach is used to predict the correspondence between geometric and material properties and the modal response. We demonstrate that machine learning is effective in predicting the mechano-acoustic behavior thus representing an inexpensive alternative with respect to finite element simulations.

Keywords: *musical acoustics, FEM, machine learning, archtop guitar*

1. INTRODUCTION

The numerical simulation of musical instruments is probably one of the fastest paced areas in contemporary musical acoustics. Modern modelling software, together with laser or computer tomography scans, allow for faithful digital reproductions of actual instruments with an excellent match in the vibrational properties of experiment and model (for a review, see [1]). However, the acoustic properties, as well as the sound of the instrument, are not directly obtainable from the vibrational properties alone. Furthermore, these accurate models are computationally expensive to evaluate and difficult to create in the first place, making them inaccessible for the average instrument maker.

In this context, using artificial intelligence (AI) to predict the acoustic behaviour of the digital model appears as a great opportunity to simplify the workflow [2–4]. Not only is it orders of magnitude faster than traditional FEM simulations, but once trained, the AI can be deployed in easy-to-use applications that do not require large computational power nor specialised knowledge from the user to be run. This consideration is reinforced by the fact that current CPUs for mobile devices are equipped with powerful computational units dedicated to artificial intelligence, thus removing the need of standard PCs for the use of such applications.

The prediction of the sound pressure level (SPL) of the instrument is a much more relevant descriptor than merely its vibrational frequencies. It is this quantity together with the mobility that one needs when one computes the sound synthesis of the instrument [5–7]. In terms of computation power it requires much more complex simulations than just the structural vibration, as is usually done in the literature, but gives a far more nuanced idea of how the instrument will actually sound. Having an AI that can accurately predict the SPL could completely transform the way we do acoustic studies of musical instruments. This is what we aim for in the following article.

The archtop guitar is an excellent test case to develop such methodology. It is a relatively simple instrument, without complicated bracing as the classical or western guitar, and its outline and arching are easy to describe with only a few parameters, in contrast to the violin family instruments whose geometry is far more complex. We hope

**Corresponding author*: tsuresuregusa@gmail.com.

this article brings more attention to an instrument that has been rather ignored by the musical acoustic community, and to the best of our knowledge, has only be studied in three articles [8–10].

2. METHODOLOGY

2.1 Geometric modelling

We realized the 3D model of the guitar body using Autodesk Fusion 360. We took the dimensions of a Gibson L-5 body, while the arching profile of the top and back plates was obtained from a scan of the upper surface of the top plate of a real archtop guitar. To model the top plate we first define the upper surface, starting from the outline and then proceeding with the arching, mimicking the one obtained from the 3D scan using one longitudinal rail and six transversal arches, see Fig. 1. The fit of the rails to the scanned surface is done by eye.

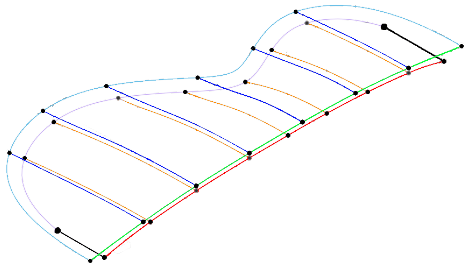

Figure 1. Upper surface: Central longitudinal rail (green line), 6 transversal rails (blue lines), outline profile (light blue curve). Lower Surface: Central longitudinal rail (red line), 7 transversal rails (orange lines), flat surface inner profile (purple curve), profile modification to accommodate for endblocks (black lines).

Then we modelled the lower surface through the definition of a flat area for the surface close to the outline and an inner arched one. The flat surface is needed for gluing the plate to the sides, linings and endblocks. We define this portion of the lower surface by creating a copy of the outline of the plate and then by offsetting it normally inward, as represented by the purple line in Fig. 1.

We then define a longitudinal rail and 7 transversal ones which are used to control the arching of the inner surface. The transversal rails are defined as splines having two control points, one on the longitudinal rail and one on the inner edge of the flat surface. We use these rails to control the arching of the inner part of the lower surface of the top plate. Finally, we build the arched portion of the lower surface using the “surface patch” tool on the rails.

To create the different top thickness models we first define the lower surface to obtain a reference plate which has thickness of 6 mm. This is possible only in the inner portion of the plate where the thickness is controlled by the arching of the lower surface. We have no possibility to control the thickness of the outer portion where we have the flat lower surface, except for the external perimeter where we can set the distance between the outline of the upper and lower surface. Once the reference top plate has been built, we assign a set of parameters to the rails that control the arching of the lower surface, obtaining a model with parametrical control of the thickness. Note that this particular model does not have a re-curve near the edge.

For the braces, the position of the face facing the bottom plate is fixed along the Z axis while the face that creates the contact area with the lower surface of the top plate depends on its arching. This leads to have an increase in the height of the braces in correspondence with the lowering of the thickness of the top plate and viceversa.

Finally, we build the sides, the endblocks, the linings, and we define the back plate by mirroring the top plate with reference thickness.

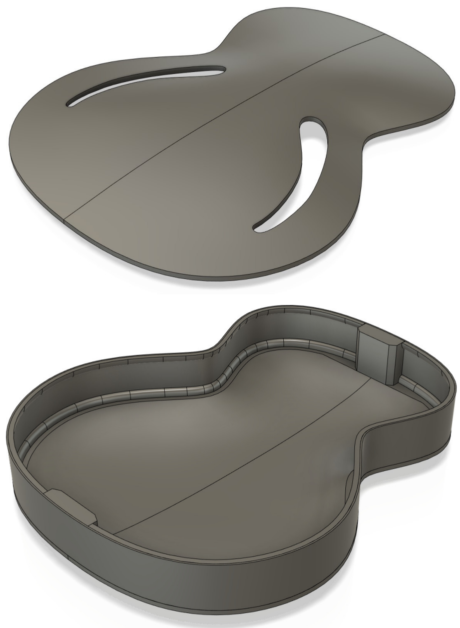

Figure 2. 3D model of the Archtop guitar body.

2.2 FEM simulations

Our FEM simulations are based on our previous studies [2, 3, 10–12] with added complexity implied by the air volume inside and outside the body of the instrument, both defined through FEM and applying spherical wave radiation boundary on the external air domain. We already implemented the air in [12] but in that case the external air was modeled through Boundary Element Method (BEM).

The 3D models have been extracted from Fusion360 and imported into Comsol as .sat files. Through the usage of this kind of file extension Comsol is able to recognize each individual component of the body independently. Once imported, we assigned a local coordinate system to every component of the body, which has made it possible to define the wood grain direction for each component separately. In the material section we have defined the wood species as orthotropic materials, assigning to them the mechanical parameters from Table 1. Notice that the material modelled here for the top plate is solid wood, as the actual guitar example, and not bent or pressed. The only exception to the aforementioned procedure has been the definition of the material used for the sides and the linings. Luthiers shape the sides through the heating and bending of thin wood plates. For this reason it is not possible to define the grain direction through a linear coordinate system. Indeed the wood fibers now follow the outline of the guitar body and no straight direction can be determined. The choice has then been to define a third material just for the sides and the linings. We have defined this material as an isotropic approximation of Red Maple. Preliminary experiments have shown that, while this approximation simplifies and solves the problem of grain orientation for the sides, it implies a very small deviation from the actual behaviour.

For the air domain, we define 2 separate regions: inside and outside the body. The separation between the two regions has been achieved using the cap faces tool in Comsol design, which generated two surfaces closing the soundholes on the top surface of the soundboard. At first we have generated a volume enclosing the guitar body. We then used the guitar body as a splitting tool to divide the volume into two domain, keeping only the one internal to the guitar.

To define the external air, we have generated a 30 cm radius sphere, centred in the middle of the guitar body, and then we have defined the domain by removing from the sphere both the guitar structure domains and the inner air domain.

Table 1. Mechanical properties of the wood used in the model and simulation, taken from [13].

Density [kg m-3]			
Engelmann Spruce	350		
Red Maple	540		
Young's Moduli [GPa]			
	E_L	E_R	E_T
Engelmann Spruce	9.79	1.25	0.58
Red Maple	12.43	1.74	0.83
Shear Moduli [GPa]			
	G_{LR}	G_{RT}	G_{LT}
Engelmann Spruce	1.21	0.10	1.17
Red Maple	1.65	0.30	0.92
Poissons's Ratios			
	ν_{LR}	ν_{RT}	ν_{LT}
Engelmann Spruce	0.422	0.53	0.462
Red Maple	0.434	0.762	0.509

We assigned the two air domains to the ”Pressure Acoustics, Frequency Domain” interface, which belongs to the Acoustics Module. This interface applies FEM to the acoustic problem. We applied a spherical wave radiation boundary condition on the surface of the sphere to model the effect of the propagation outside of the modelled portion of space. Preliminary experiments confirmed that the model spherical wave radiation does not introduce artifacts to the sound pressure level, especially in terms of reflections coming back from the boundaries of the air domain.

At last we have assigned the built-in Air material to the two air domains and meshed them using free tetrahedral elements.

For each guitar body simulated we have conducted two different studies: first, the eigenfrequencies of the whole system have been computed. Then, taking only the first 5 eigenfrequencies, we compute the amplitude of the mobility at the bridge position, when exciting the guitar at the location of the treble foot of the bridge, and of the sound pressure level at a point 20cm above the center of the top plate. Computing the complete SPL as a function of frequency is only computationally more expensive but conceptually the same as this, we thus leave that study for a future work.

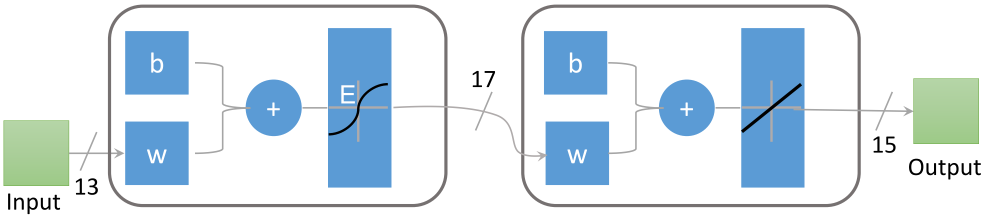

Figure 3. Architecture of the NN used to predict the frequency and amplitude. We have used a one hidden layer neural network with dimension 13 in the input, 17 neurons in the hidden layer, and 15 dimensions for the output. The activation function for the hidden layer is an Elliot sigmoid, whereas for the output layer is a linear function.

2.3 Dataset generation

The dataset is generated by random sampling the material parameter space with a gaussian distribution centred in the nominal values of the material parameters for spruce. We assume that each parameter is independent, which may not be a realistic assumption considering that in nature there is a slight correlation between the density of the wood and other mechanical parameters [14].

The center values of the material parameters correspond to the nominal elastic constants of *Engelmann spruce* as reported in Table 1. The center value of the density is set to $\rho_0 = 350$ $[\text{Kg m}^{-3}]$. There is only one geometrical parameter that controls the thickness of the plate, and is varied discontinuously between +2mm and -2mm maximum thickness variation of the top plate, varying the control parameter in steps of 5% increments. The standard deviation of the Gaussian random variables δ_Y is $\sigma_M = 0.25$ for the elastic parameters, $\sigma_\rho = 0.1$ for the density. It's worth noticing that these parameters for the random sampling generate a distribution of material parameters far larger than the one actually found in instrument making. In particular, the maximum stiffness is more than 3 times the minimum stiffness, whereas in experiments the range is found to be just twice [15].

We model the damping of the plate by means of the Rayleigh damping model [16] and set its two control parameters $\alpha = 0$ $[\text{s}^{-1}]$ and $\beta = 2 \times 10^6[\text{s}]$. Despite not being very realistic, it is a model commonly used in the literature [1].

At the end of the whole process, we obtain a dataset of 270 occurrences with 13 inputs (i.e. 9 elastic constants, one geometry parameter, the density and the 2, fixed, damping parameters) and 10 outputs. The outputs are the frequency/mobility/SPL triplets corresponding to the first 5 eigenfrequencies.

2.4 AI architecture and training

In order to predict the eigenfrequency f_s, the mobility amplitude m_s and the Sound Pressure Level SPL_s, we employ a Single-layer Feedforward Neural Networks [17]. We choose to employ these networks since they are reckoned to be universal approximators of general mappings from one finite dimensional space to another [18].

The *Matlab*® Machine Learning Toolbox NNTRAINTOOL [19, 20] is used to implement and train the MFNN following the Levenberg-Marquadt algorithm [21]. We have used a one hidden layer neural network with dimension 13 in the input, 17 neurons in the hidden layer, and 15 dimensions for the output. The activation function for the hidden layer is an Elliot sigmoid, whereas for the output layer is a linear function.

To train and test the neural network, we randomly split the dataset into train set and test set containing the 90% and the 10% of the total occurrences, respectively.

3. RESULTS

Figure 4 shows two examples of the dependence of the frequency and amplitude of the mobility's first peak for different longitudinal stiffnesses. The data is obtained from the complete dataset and has values of stiffness ranging from 3 GPa to 19 GPa, randomly sampled according to the distribution described in section 2. The range of frequencies in which the first peak varies is quite significant, going from the low 170Hz up to 190Hz. The amplitude of the peak shows a variation of almost 20dB, showing how relevant the variation in material parameters is for the sound production of the instrument. From the scatter

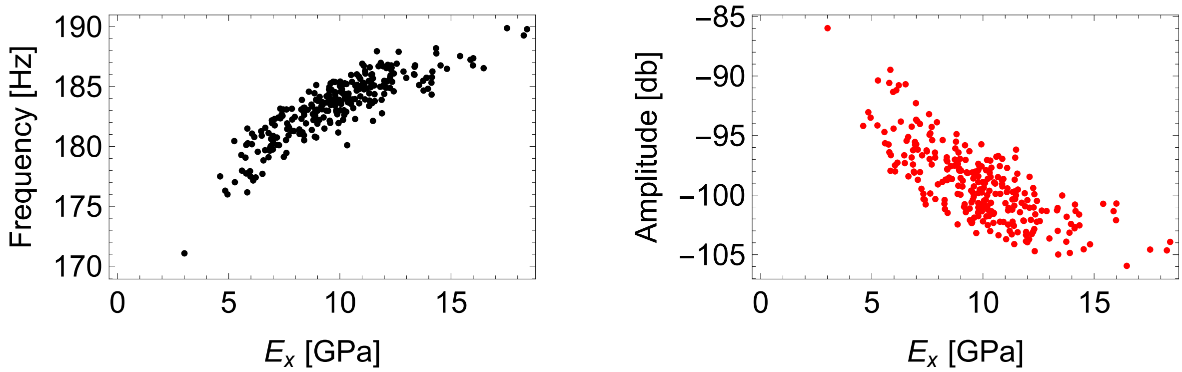

Figure 4. Frequency (left) and amplitude (right) of the first peak as a function of the longitudinal stiffness of the top plate for 270 simulations.

plots it is clear that there is a negative correlation between the frequency and the amplitude of the first peak: higher is the frequency, lower is the amplitude. It is worth noticing that the variation in stiffness is far larger than the one reported experimentally [15] so if the NN is able to predict in this dataset the results should be valid as well in real instruments.

Figure 5 shows the predicted versus actual values for the frequency, mobility amplitude, and SPL evaluated in the test set. The mean coefficient of determination, R^2, for the 15 variables is $< R^2 >\simeq 0.93$. As it can be seen from the data, the fit is almost perfect for the frequency $R_f^2 = 0.96$, slightly worse for the mobility $R_m^2 = 0.95$ (in particular mode 4). and rather poorly for the SPL with an $R_s^2 = 0.86$. The mode with the maximum error, the third mode, is a very low $R_{s3}^2 = 0.76$.

If one thinks of sound in terms of the propagation of a surface field in a 3D space [22] the larger error in the prediction of the SPL is not surprising. The pressure in one point of the space is the integral of the propagated contributions of each point on the surface of the guitar. Thus, learning the SPL is equivalent to somehow learning the mobility for each point of the instrument. Obviously, a network that has enough expressivity to learn the mobility at one point of the instrument without overfitting, won't be able to accurately learn all the points of the instrument. It stands to reason then that to learn the SPL in an accurate manner a more complex architecture and more data are required.

To study this dependence in the complexity of the network we trained different architectures (both increasing the layers and splitting the prediction per physical quantity), but the results were all worse than the one presented here due to overfitting. In the future we will augment the dataset to avoid this issue and find a better performing network.

A final mention of the speed up is worth making here: the FEM simulation first needs to compute the eigenfrequencies and then the admittance and SPL at those frequencies to compute the amplitudes. In total this takes about five minutes. When using the AI the computation only takes 0.05 s, which results in a speed up of 6000X once the training has been done, which in our case took 2 days of continuous computation.

4. CONCLUSIONS

In this article we have shown that a NN can accurately predict the frequency and amplitude of the first five peaks in the mobility response of a full 3D model of an archtop guitar. The ground truth results are obtained from a multiphysics simulation involving the structure of the instrument as well as the air volume in and around it.

Despite the simplicity of the NN, the prediction is extremely fast and accurate for both the frequency of the peaks and the mobility amplitude. After the training is done, evaluating the NN has practically a zero computational cost, allowing for the fast prediction of different designs and materials and their influence in the sound of the instrument. This could be easily implemented in a way that is easy to use for instrument makers.

We have also looked into the prediction of the sound

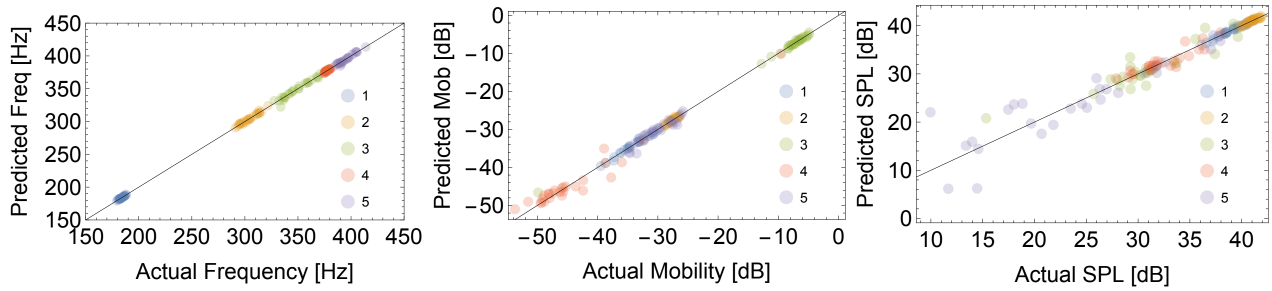

Figure 5. Predicted versus actual eigenfrequencies, mobility and SPL for the test dataset for each of the modes, labeled from 1 to 5 in the legend.

pressure level with less accurate, but reasonably good, results. The fact that the error in the prediction increases as we try to predict more complex observables is expected. From our previous research [4] we know that for the simpler case of a rectangular plate, different architectures are optimal for the prediction of the frequency and the amplitude of the peaks in the mobility simulations, the network needed for the amplitudes is of a larger complexity than the one needed for the frequency. It stands to reason that predicting the SPL requires an even more complex architecture since the results are a propagation of the mobility in the whole surface of the instrument, not in a single point. Doing a complete hyperparameters optimisation goes far beyond the scope of this paper but is a promising research question that we are currently investigating.

One surprising result is that the complexity of the network needed to predict the frequencies and amplitudes of the mobility for the complete guitar is less than for ”simpler” systems such as the plates already mentioned [4]. The reason for this is that by isolating the effect of the top plate, and coupling it with a guitar body of fixed geometry and materials, we are actually reducing the impact that the top plate has on the complete instrument [12]. We speculate that a complete variation of the materials of the instrument would require a more complex architecture yet it would be conceptually equivalent.

For the sake of simplicity, we have focused in this article only in the frequency and amplitude of the response. Current artificial sound synthesis model require the full modal characterisation, that is, also the damping for each peak. We are confident that this algorithm will work as well with the prediction of the complete SPL (or a modal approximation of it) and could be used to — in real time — hear the sound of a virtual instrument. This is another step in that direction.

5. REFERENCES

[1] E. Kaselouris, M. Bakarezos, M. Tatarakis, N. A. Papadogiannis, and V. Dimitriou, “A review of finite element studies in string musical instruments,” in *Acoustics*, vol. 4, pp. 183–202, MDPI, 2022.

[2] S. Gonzalez, D. Salvi, D. Baeza, F. Antonacci, and A. Sarti, “A data-driven approach to violin making,” *Scientific reports*, vol. 11, no. 1, pp. 1–9, 2021.

[3] D. Salvi, S. Gonzalez, F. Antonacci, and A. Sarti, “Parametric optimization of violin top plates using machine learning,” *arXiv preprint arXiv:2102.07133*, 2021.

[4] D. G. Badiane, R. Malvermi, S. Gonzalez, F. Antonacci, and A. Sarti, “On the prediction of the frequency response of a wooden plate from its mechanical parameters,” in *ICASSP 2022 - 2022 IEEE International Conference on Acoustics, Speech and Signal Processing (ICASSP)*, pp. 461–465, 2022.

[5] M. Rau, J. S. Abel, D. James, and J. O. Smith III, “Electric-to-acoustic pickup processing for string instruments: An experimental study of the guitar with a hexaphonic pickup,” *The Journal of the Acoustical Society of America*, vol. 150, no. 1, pp. 385–397, 2021.

[6] G. O. Paiva, F. Ablitzer, F. Gautier, and J. M. C. dos Santos, “Collisions in double string plucked instruments: Physical modelling and sound synthesis of the viola caipira,” *Journal of Sound and Vibration*, vol. 443, pp. 178–197, 2019.

[7] G. O. Paiva, M. Queiroz, and M. R. Machado, “Study of the influence of wood mechanical properties variability on the sound synthesis of a simplified string instrument,” in *Recent Trends in Wave Mechanics and*

Vibrations: Proceedings of WMVC 2022, pp. 890–899, Springer, 2022.

[8] M. French, "Dynamics of an archtop jazz guitar," in *Proceedings, 21st International Modal Analysis Conference, Orlando*, 2003.

[9] T. J. Nania, "Archtop guitar dynamics," *Violin Society of America Papers*, vol. 29, no. 1, pp. 1–13, 2021.

[10] D. Salvi, S. Gonzalez, F. Antonacci, and A. Sarti, "Modal analysis of free archtop guitar top plates," *The Journal of the Acoustical Society of America*, vol. 150, no. 2, pp. 1505–1513, 2021.

[11] S. Gonzalez, D. Salvi, F. Antonacci, and A. Sarti, "Eigenfrequency optimisation of free violin plates," *The Journal of the Acoustical Society of America*, vol. 149, no. 3, pp. 1400–1410, 2021.

[12] M. Lercari, S. Gonzalez, C. Espinoza, G. Longo, F. Antonacci, and A. Sarti, "Using mechanical metamaterials in guitar top plates: a numerical study," *Applied Sciences*, vol. 12, no. 17, p. 8619, 2022.

[13] R. J. Ross *et al.*, *Wood handbook: Wood as an engineering material*. The Laboratory, 2010.

[14] R. Viala, *Towards a model-based decision support tool for stringed musical instruments making*. PhD thesis, Bourgogne Franche-Comté, 2018.

[15] S. Merchel, M. E. Altinsoy, and D. Olson, "Perceptual evaluation of bracewood and soundboard wood variations on the preference of a steel-string acoustic guitar," *The Journal of the Acoustical Society of America*, vol. 146, no. 4, pp. 2608–2618, 2019.

[16] J. Rayleigh, *The Theory of Sound, Volume One*. Dover Books on Physics, Dover Publications, 2013.

[17] D. Svozil, V. Kvasnicka, and J. Pospichal, "Introduction to multi-layer feed-forward neural networks," *Chemometrics and intelligent laboratory systems*, vol. 39, no. 1, pp. 43–62, 1997.

[18] K. Hornik, M. Stinchcombe, and H. White, "Multilayer feedforward networks are universal approximators," *Neural networks*, vol. 2, no. 5, pp. 359–366, 1989.

[19] M. H. Beale, M. T. Hagan, and H. B. Demuth, "Neural network toolbox user's guide," *The MathWorks Inc*, vol. 103, 1992.

[20] F. Aldakheel, R. Satari, and P. Wriggers, "Feed-forward neural networks for failure mechanics problems," *Applied Sciences*, vol. 11, no. 14, pp. 64–83, 2021.

[21] J. J. Moré, "The levenberg-marquardt algorithm: implementation and theory," in *Numerical analysis*, pp. 105–116, Springer, 1978.

[22] M. Moosrainer and H. Fleischer, "Application of bem and fem to musical instruments," *Boundary Elements in Acoustics*, pp. 377–410, 2000.